Electron Crystallography and Organic Materials with Non-linear Optical Properties

Ingrid G. Voigt-Martin[1]*, Ute Kolb[1], Hans Kothe[1],
Alexander V. Yakimanski[1,2], Ri-Cheng Yu[1], Galina N. Matveeva[1,2],
Andrey V. Tenkovtsev[2]

[1]Institut für Physikalische Chemie der Universität Mainz,
Jakob Welder Weg 11, D-55099 Mainz, Germany
[2]Institute of Macromolecular Compounds of the Russian Academy of Sciences,
Bolshoi pr. 31, 199004 St. Petersburg, Russia

SUMMARY: Results of electron microscopic studies of crystal structures of a number of bis-benzylidene cyclohexanones are presented. It is shown that some of these compounds are efficient crystalline non-linear optically active (NLO) chromophores with second harmonic generation (SHG) properties. Appropriately functionalized chromophores of this type can be used as a polycondensation comonomer to produce partly crystalline main-chain NLO-active polymers. Electron diffraction crystal structural data, obtained for very small crystals, allowed us to get reasonable estimations of macroscopic crystal NLO-coefficients, relating quantum-chemically calculated molecular first hyperpolarizability components to crystal axes.

Introduction

Electron microscopic investigations of beam sensitive, organic molecules have reached considerable sophistication in recent years due to the combined application of quantum mechanics, simulation methods and maximum entropy statistics. However, even beyond the determination of atomic positions in the unit cell, it is possible to calculate specific physical properties of small organic molecules from quantum chemical calculations of molecular parameters and to relate these to the crystal axes. In cases where crystals are too small for X-ray analysis, electron crystallography is the only way to obtain this information.

Our procedure requires close collaboration between organic chemists, quantum chemists, and electron crystallographers. It can be summarized as follows[1-5]:

1) Crystals are grown from solution and screened for NLO effect.
2) Electron diffraction patterns are obtained and intensities are quantified.
3) Diffraction patterns are simulated using packing energy calculations and an initial gas-phase molecular conformation is calculated by quantum chemical methods.

 CCC 1022-1360/99/$ 17.50+.50/0

4) High resolution images are improved by image restoration and simulated using multislice methods.
5) Dynamic scattering contributions are calculated.
6) *Ab initio* structure determination using Maximum Entropy approach is performed and independently compared with the model.
7) Molecular first hyperpolarizability tensor components are either calculated, using quantum-chemical methods, or measured in solution, employing EFISH (Electric Field Induced Second Harmonic Generation) and Hyper Rayleigh Scattering methods, and are related to crystal coordinates to estimate macroscopic NLO-susceptibility.

Samples

The samples consist of a series of different bis-benzylidene cyclohexanones presented below:

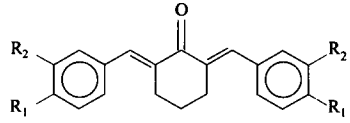

2,6-bis(4-hydroxy-benzylidene)-cyclohexanone (**BHBC**, R_1= –OH, R_2= –H), 2,6-bis(4-dimethylamino-benzylidene)-cyclohexanone (**DMABC**, R_1= $-N(CH_3)_2$, R_2= –H), 2,6-bis(3-methoxy-4-hydroxy-benzylidene)-cyclohexanone (**BMHBC**, R_1= –OH, R_2= $-OCH_3$), and the polymer, obtained by polycondensation of **BMHBC** with sebacinoyl chloride, $ClOC-(CH_2)_8-COCl$, poly-[sebacinoyl-2,6-bis(3-methoxy-4-oxy-benzylidene)-cyclohexanone] (**PSBMOBC**, R_1= $-OCO-(CH_2)_4-$, R_2= $-OCH_3$).

Methods

A. Quantum chemical calculations

The quantum chemical calculations are required to calculate the molecular conformation and to calculate molecular first hyperpolarizability β-tensor components related to crystal quadratic non-linearity d-tensor via eqn. (1):

$$d_{IJK}(-2\omega;\ \omega_1,\omega_2) = (N/V)[f_I\ (2\omega)\, f_J\ (\omega)\, f_K\ (\omega)\ \Sigma\Sigma\ \cos\theta_{Ii}\ \cos\theta_{Jj}\ \cos\theta_{Kk}\ \beta_{ijk}] \qquad (1)$$

where N is the number of molecules in the unit cell of volume V, f_I are local-field factors and θ_{Ii} defines the angle between the molecular *i*-axis and crystal *I*-axis.

For all the above molecules, a minimum energy gas phase geometry was generated[6-8], using both semi-empirical PM-3[9] methods implemented in the MOPAC 6.0 program[10] and the Density Functional Theory (DFT) *ab initio* approach[11] implemented in the TURBOMOLE program package[12]. The details concerning basis sets used for the DFT-calculations were described earlier[6].

The PM-3 method was used for calculations of static molecular polarizabilities. The TURBOMOLE program was employed for *ab initio* calculations of both static and frequency-dependent α tensors which are needed for the estimation of frequency dependent local-field factors $f_I(\omega)$ in eqn.(1). The *ab initio* α-tensor calculations were performed with the 6-31G*(+) basis set specially optimized for molecular polarizability calculations[13].

B. Structure determination

Single crystal electron diffraction data were obtained with a Philips transmission electron microscope, using a rotation-tilt holder in order to obtain diffraction patterns from suitable crystallographic zones and a low dose unit to reduce beam damage. For subsequent quantitative analysis it is essential to produce both tilt and exposure series. Experimental details have been described previously[1-5].

C. Quantifying electron diffraction patterns

The diffraction data are scanned with a Nikon LS 4500 scanner at a resolution of 3000 d.p.i. and transferred to a PC for quantifying using the ELD software[14]. It is essential to ensure that ELD is evaluating the intensities correctly and to use exposure series[15]. If on-line CCD facilities are available intensity evaluation can be considerably improved[7].

The quantitative values are initially compared with those expected kinematically from the model (next paragraph) and assessed by calculating the R-factor.

D. Simulation of diffraction patterns

On the basis of the cell parameters and space group calculated from the electron diffraction patterns and a calibration X-ray powder pattern, an initial model is built up in CERIUS 2.0[16]. Packing energy calculations were performed using the crystal packer module. This is a force-field approach, with the limitations pointed out previously[17]. For the molecules studied here,

the optimal gas phase conformation of the cyclohexanone moiety can differ from the exact crystal state conformation[7,8]. Such differences cannot be removed by crystal packer because it does not optimize subrotations within cyclic molecular fragments. In addition, the effect of intermolecular H-bonds between molecules in the crystal state cannot be taken into account by gas-phase calculations of an isolated molecule.

In order to avoid positive packing energies and to provide the most favorable intermolecular H-bonding, slight adjustments to torsional angles were necessary in all cases[1-8,17].

The electron diffraction patterns from all zones as well as the X-ray powder pattern were simulated and refined against experimental data. After several cycles between minimization of the packing energy and comparison against experimental electron diffraction data, model structures were obtained and the R-factor calculated. Macroscopic NLO-coefficients may then be calculated, using eqn. (1), and predictions can be made regarding the suitability of a specific molecule for SHG-applications[1-8].

E. The maximum entropy approach

The solution of structures of this complexity using the standard direct methods as in X-ray crystallography is often not possible. A major problem is related to the fact that the number of available reflections is too small, particularly in the high angle region. We have discussed previously why the maximum entropy method in a crystallographic environment, first proposed by Bricogne[18] and subsequently developed by Bricogne and Gilmore[19], has proved to be extremely powerful in connection with limited data sets such as those obtained by electron diffraction[1-8].

F. Dynamic scattering effects

Dynamic scattering effects must always be accounted for in electron diffraction investigations. In the past we have used the multislice calculations[20] available in CERIUS. When using on-line CCD facilities for recording diffraction patterns, we have found it convenient to use the MSLS program[7,8].

Results

Clearly it is not possible to present the results obtained for all the molecules investigated in detail. However, general trends and certain highlights can be mentioned here:

A. Quantum chemical calculations

For all the molecules in question semi-empirical calculations tended to give a bent molecular conformation while *ab initio* calculations indicated that the molecule is almost flat. As an example, we show the **DMABC** molecule in Fig. 1. The other molecules in the series are discussed elsewhere[6-8].

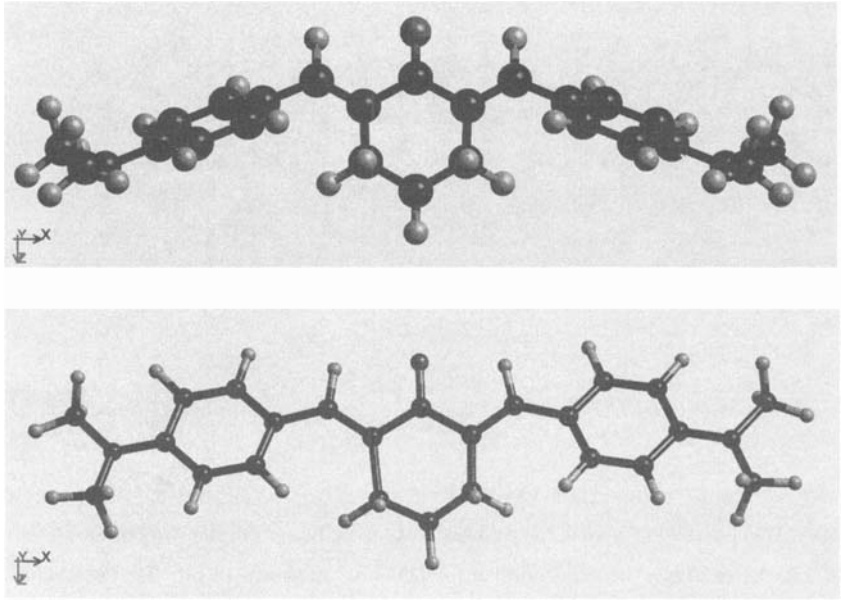

Fig. 1. Gas phase conformation of DMABC molecule calculated by semi-empirical PM-3 method (above) and by DFT *ab initio* approach (below).

B. Crystal structure determination

For all the molecules in the series it was possible to obtain the cell parameters and space group from the series of electron diffraction patterns. In all cases the cell parameters were refined using X-ray powder data. The space groups are: $Cmc2_1$ for **DMABC**, $Pna2_1$ for **BHBC**; $P2_1/c$ for **BMHBC**; $P2_111$ for **PSBMOBC**. Of these, only **BMHBC** is centro-symmetric, thus excluding an SHG-effect from the start.

In all cases it was possible to obtain reasonable packing energies. These tended to be ~ –200 kcal/mol/unit cell. The major contribution in all cases was the Van der Waals energy. As an

example, we show the [010]-projection of the **DMABC** crystal structure in Fig. 2. The R-factors before correction for dynamic scattering were in the region of 30%. Although such a value is unacceptable in X-ray scattering, this is reasonable for electron diffraction before correction for dynamic scattering. After corrections for dynamic scattering, Ewald sphere, centre of Laue circle it was possible to reduce this number to 17%[7,8].

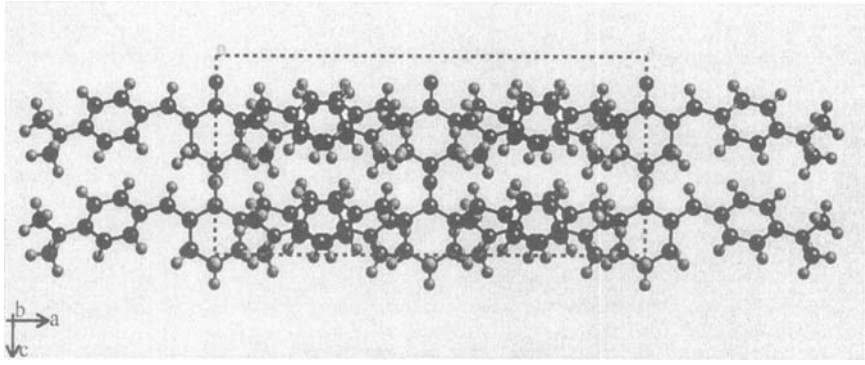

Fig. 2. Crystal structure of **DMABC** obtained by packing energy minimization procedure[7].

C. Maximum entropy structure determination

In all cases it was possible to obtain centroid maps showing the molecular orientation in the unit cell[1-8]. As an example, the centroid map for **DMABC** is shown in Fig. 3. These maps clearly indicate that the simulated structure is correct and reflect the molecular contours within the unit cell. While the maps can produce only low resolution because of the missing data, the simulations give the atomic positions, thus enabling physical parameters to be calculated.

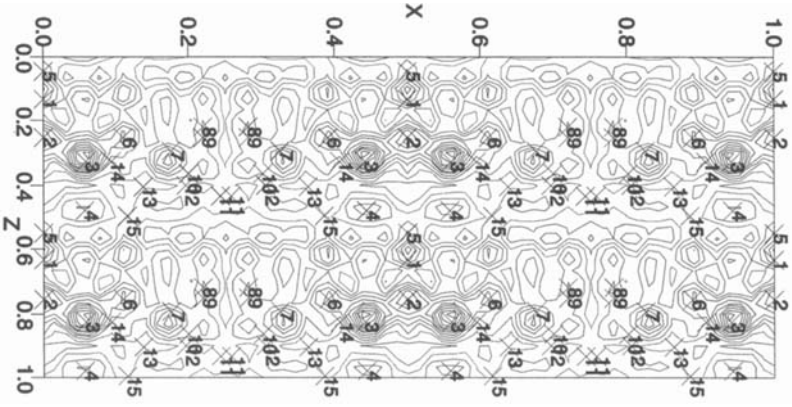

Fig. 3. Centroid map for **DMABC** corresponding to the [010]-projection in Fig. 2.

D. Results for polymer

Using CERIUS 2.0 simulations, the NLO-active polymer **PSBMOBC** was found to crystallize in an orthogonal unit cell with monoclinic symmetry (unique a-axis):

Space group $P2_111$; Z=2; d=1.05 g/cm^3; a= 7.4 Å; b=11.3 Å; c=19.6 Å; α=90°.

The projection of the proposed polymer crystal structure along the monoclinic a-axis is shown in Fig. 4. In order to solve this structure, $P2_1/c$ crystal structure of the low molecular weight analog BMHBC[8] was used as an initial model. For the polymer model, the cycles of cell parameters refinement and crystal packing energy minimization were performed until a reasonable agreement between the simulated and experimental X-ray powder diffraction and favorable packing energy (ca. –70 kcal/mol/cell) was achieved. The molecule exhibits a zig-zag conformation and segregation of the aliphatic and aromatic parts (Fig. 4).

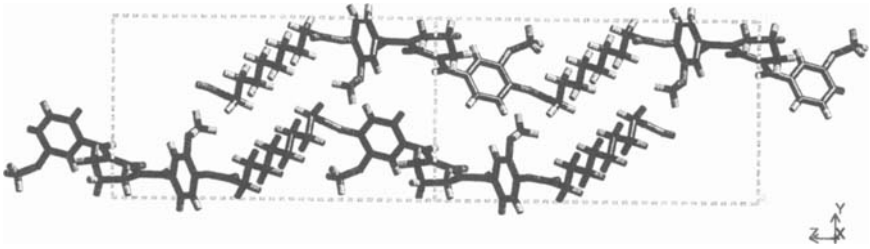

Fig. 4. Simulated crystal structure of the NLO-active polymer **PSBMOBC**.

E. Calculation of non-linear optical parameters

Of the molecules in the series discussed here, by far the largest value of 111 pm/V for the effective NLO-coefficient was measured for **DMABC**[21]. The structure analysis for **DMABC** shows that the dipole moments of different molecules (parallel to their C=O double bonds) in the unit cell are predominantly oriented along the *c*-direction (crystal *Z*-axis). As the π-conjugation in all molecules is mainly along the *a*-direction (crystal *X*-axis), this gives rise to a considerable resultant macroscopic quadratic susceptibility with dominating two-dimensional contribution from the d_{ZXX} NLO-coefficient. Our PM-3 estimations for the **DMABC** crystal d_{ZXX} NLO-coefficient gave the value of 35.7 pm/V[4].

The individual values for the other NLO-active crystals is published elsewhere[6,7]. In almost all of them, although non-centrosymmetric, the molecular arrangement is not so favorable for high SHG-efficiency and most of the larger molecular β-tensor components from different molecules in the unit cells compensate for each other.

A comparison of the conformations obtained by *ab initio* gas phase calculations and those obtained in the crystal indicate the complexity of the crystal field effects. While only very small molecular rotations of the end groups distinguished the gas-phase conformation of **DMABC** and **BHBC** from that in the crystal, **BMHBC** showed a slightly larger difference. It is likely that H-bond effects are responsible for this.

In the **PSBMOBC** crystal structure (Fig. 4), C=O double bonds of the backbone NLO-chromophore groups form an angle α=28° with the screw a-axis. Such an arrangement is rather favorable for displaying an SHG-effect, the d_{XZZ} NLO-coefficient being mainly promoted (the assignment of axes corresponds to the crystal structure shown in Fig. 4). The expression for d_{XZZ} may be derived from eqn. (1) as[22]:

$$d_{XZZ} = (N/V)\, f_X\, (f_Z)^2 \beta_{yxx} \cos\alpha \qquad (2)$$

It should be noted that in the polymer crystal structure, phenyl rings are arranged perpendicularly with respect to the planes of C=C double bonds on both sides of the central cyclohexanone fragment. Therefore, π-conjugation between the C=C double bonds and phenyl rings is absent, resulting in a decrease of the major β_{yxx}-component of the molecular first hyperpolarizability tensor. PM-3 estimations of local-field factors, using linear polarizability tensor components related to the crystal axes[4], gave f_X = 1.305 and f_Z = 1.421. Using the PM-3 calculated value of $\beta_{yxx} = 2.5 \cdot 10^{-30}$ e.s.u. in eqn. (2), predicted d_{XZZ} value for the perfect crystal is $7.0 \cdot 10^{-9}$ e.s.u. = 2.9 pm/V. However, the observed polymer powder

SHG-efficiency seems to be strongly reduced due to the poor crystallinity of the polymer sample.

Conclusion

It has been shown that a detailed analysis of crystal quadratic non-linearity tensor components is possible based on electron diffraction data. Such an analysis shows which molecules are possible candidates for a well directed design of materials with specific physical properties. In particular, for the design of polymers it is important to know the conditions enabling optimization of the physical properties. For this series of molecules it appears that the mirror plane in **DMABC** combined with a centered cell had the effect of maximizing the resultant crystal SHG-effect. It was recently suggested[23] that the driving force for highly SHG-effective non-centrosymmetric crystallization of bis-benzylidene-cycloalkanones is carbonyl oxygen attractive interaction with methylene protons of cycloalkanone moieties. Such attractive interactions (similar to weak H-bonds) are destroyed by *o*- or *m*- substitution in the benzylidene fragment[23] (centrosymmetric crystal structure of **BMHBC**).

Acknowledgements

The authors are thankful to Deutsche Forschungsgemeinschaft for financial support.

References

1) I. G. Voigt-Martin, D. H. Yan, A. Yakimansky, D. Schollmayer, C. J. Gilmore, G. Bricogne, *Acta Cryst.* **A51**, 849 (1995)
2) I. G. Voigt-Martin, Li Gao,A. Yakimanski, G. Schulz, J .J. Wolff, *J.Amer.Chem.Soc.* **118**, 12830 (1996)
3) I. G. Voigt-Martin, Z. X. Zhang, D. H. Yan, A. Yakimanski, R. Wortmann, R. Matschiner, P. Krämer, C. Glania, N. Detzer, *Colloid and Polymer Science* **275**,18 (1997)
4) A. V. Yakimanski, U. Kolb, G. N. Matveeva, I. G. Voigt-Martin, A. V. Tenkovtsev, *Acta Cryst.* **A 53**, 603 (1997)
5) I. G. Voigt-Martin, Z. X. Zhang, U. Kolb, C. Gilmore, *Ultramicroscopy* **68**, 43 (1997)
6) I. G. Voigt-Martin, Gao Li, U. Kolb, H. Kothe, A.V. Yakimanski, A. V. Tenkovtsev, C. Gilmore, *Phys. Rev.* **B59**, 6722 (1999)
7) I. G. Voigt-Martin, H. Kothe, A. V. Yakimanski, A. V. Tenkovtsev, H. Zandbergen, J. Jansen, C. Gilmore, *Ultramicroscopy* (submitted)
8) R. C. Yu, A. Yakimanski, H. Kothe, I. G. Voigt-Martin, C. Gilmore, J. Jansen, H. Zandbergen, A. V. Tenkovtsev, *Acta.Cryst.* **B** (submitted)
9) J. J. P. Stewart, *J. Comput. Chem.* **10**, 209 (1989)
10) J .J. P. Stewart, *MOPAC 6.0, A General Purpose Molecular Orbital Package*, QCPE (1990)
11) R. G. Parr, W. Yang, *Density-functional theory of atoms and molecules*, Oxford Univ. Press: Oxford (1989)
12) R. Ahlrichs, M. Bär, M. Häser, H. Horn, C. Kölmel, *Chem. Phys. Lett.* **162**, 165 (1989)
13) M. A. Spackman, *J. Phys. Chem.* **93**, 7594 (1989)
14) S. Hovmöller, *Ultramicroscopy* **41**, 121 (1992)
15) H. Kothe, U. Kolb, In: NATO ASI series: Electron crystallography Vol. 347, D. Dorset, S. Hovmöller, X. Zou, Eds., Kluwer, Dordrecht 1997, p. 383
16) Cerius2 User Guide, Month 1996. San Diego: Molecular Simulations, 1996.
17) I. G. Voigt-Martin, Gao Li, A. Yakimanski, J. J. Wolff, H. Gross, *J. Phys. Chem.* **101**, 7265 (1997)
18) G. Bricogne, *Acta Cryst.* **A40**, 410 (1984)
19) G. Bricogne, C. J. Gilmore, *Acta Cryst.* **A46**, 284 (1990)
20) J. M. Cowley, A. F. Moodie, *Acta Cryst.* **10**, 609 (1957)
21) J. Kawamata, K. Inoue, *Mol. Cryst. Liq. Cryst.* **278**, 117 (1996)
22) J. Zyss, J. L. Oudar, *Phys. Rev.* **A26**, 2028 (1982)
23) J. Kawamata, K. Inoue, T. Inabe, *Bull. Chem. Soc. Jap.* **71**, 2777 (1998)